Elevated and Deregulated Expression of HDAC3 in Human Astrocytic Glial Tumours

(cancer / HDAC3 / histone / deacetylase / glioma)

P. Libý[1], M. Kostrouchová[1], M. Pohludka[1], P. Yilma[1], P. Hrabal[4], J. Sikora[3], E. Brožová[2], M. Kostrouchová[2], J. E. Rall[5], Z. Kostrouch[1]

[1]Laboratory of Molecular Pathology, [2]Laboratory of Molecular Biology and Genetics, [3]Institute of Inherited Metabolic Disorders, 1st Faculty of Medicine, Charles University, Prague, Czech Republic
[4]Department of Pathology, Central Military Hospital Střešovice, Prague, Czech Republic
[5]National Institute of Diabetes and Digestive and Kidney Diseases, National Institutes of Health, Bethesda, MD, USA

Abstract. Abnormal expression of histone deacetylases may contribute to the establishment of a cancer specific transcription profile. We examined expression of HDAC3 in human non-malignant gliosis and glial astrocytic tumours. Samples from four non-malignant gliosis and 17 astrocytic gliomas (six of grade II, one of grade III and ten of grade IV) removed for therapeutic purposes were assayed for HDAC3 expression at mRNA and protein levels. HDAC3 mRNA was detected in non-tumorous gliosis as well as in all examined glial tumours. Seven out of eleven examined high-grade tumours showed an elevated number of copies of HDAC3 mRNA. Western blot analysis detected high levels of expression of HDAC3 in the majority of the examined tumours. Immunohistochemistry and immunofluorescence made on a collection of 35 astrocytic tumours detected nuclear as well as cytoplasmic HDAC3 expression in all of those tumours. While the distribution of HDAC3 was both nuclear as well as cytoplasmic and moderate in intensity in non-malignant tissues and low-grade gliomas, high-grade tumours expressed HDAC3 in a focally deregulated pattern that included strongly pronounced cytoplasmic localization. Confocal microscopy and additional co-localization analysis detected nuclear HDAC3 in all tumours examined. We conclude that HDAC3 expression is elevated in human astrocytic tumours and its expression pattern is deregulated at the cellular level in high-grade gliomas.

Received May 16, 2006. Accepted May 23, 2006

This work was supported by grant NC 7554-3 from the Internal Grant Agency of the Ministry of Health of the Czech Republic.

Corresponding author: Zdeněk Kostrouch, Laboratory of Molecular Pathology, Institute of Inherited Metabolic Disorders, 1st Faculty of Medicine, Charles University, Ke Karlovu 2, 128 01 Prague 2, Czech Republic, Phone (+420) 224 967 090, Fax. (+420) 224 967 119, e-mail: zdenek.kostrouch@lf1.cuni.cz

Abbreviations: DAPI – 4'6-diamidino-2-phenylindole; FFPE – formaldehyde-fixed paraffin-embedded; G – gliosis; HAT – histone acetyl transferase; HDAC – histone deacetylase; HGG – high-grade gliomas; LGG – low-grade gliomas; SAHA – suberoylanilide hydroxamic acid; T-PBS – 1% Tween 20 in phosphate-buffered saline pH 7.4; TSA – trichostatin A.

Cancer growth and behaviour, in addition to genetic changes that induce loss or gain of gene function, depend on cancer-specific transcription. The behaviour of cancer cells is fundamentally affected by a wide range of repressed genes and other sets of upregulated genes that form together a cancer-specific transcriptome (Kioussis and Festenstein, 1997; Wolffe and Matzke, 1999). Gene transcription is regulated at several levels. Genomic regions may be excluded from transcription by organizing chromatin in such a way to make it inaccessible to transcription factors and co-factors. The cell lineage depends in part on this transcriptionally inaccessible chromatin (Higgs et al., 2006). Gene expression further depends on general and cell- and tissue-specific transcription factors and co-factors.

In addition to the formation of sterically active or repressive transcription complexes, the transcription complexes bind enzymes that modify chromatin proteins. Molecular regions of histones H2A, H2B, H3 and H4 are enzymatically modified. These posttranslational modifications include acetylation, phosphorylation, methylation, ubiquitination, biotinylation and other modifications (Nightingale et al., 2006). Non-histone proteins (including constituents of transcription complexes) are also often enzymatically modified (Fu et al., 2004). Enzymatic modifications may dramatically alter protein-protein interactions, the stability of the DNA-nucleosome structure and the accessibility of transcription regulatory proteins to DNA. Acetylation of lysines predominantly localized at the N-termini of nucleosomal histones H3 and H4 is generally associated with transcriptionally active chromatin (Jenuwein and Allis, 2001). Transcription factors, such as nuclear hormone receptors associated with their agonistic ligands, bind

co-activators displaying histone acetylation activity or binding histone acetyl transferases (HATs) that directly acetylate lysines of nucleosomal histones. Acetylation can be enzymatically reversed by histone deacetylases (HDACs), which are often constituents of repressive transcription complexes. Transcription-repressing complexes that include nuclear hormone receptors in their unliganded status bind nuclear hormone receptor co-repressors SMRT and NCoR; these co-repressors bring histone deacetylases to the promoters of regulated genes and function as repressors (Zamir et al., 1996; Heinzel et al., 1997; Chen et al., 2005).

To date, two major protein families possessing histone deacetylation activity were identified. The first family includes HDAC class I and II (de Ruijter et al., 2003) and the second HDAC class III, a Sir2 family of NAD^+-dependent protein deacetylases, called sirtuins (Grubisha et al., 2005). HDAC class I consists of HDAC1, HDAC2, HDAC3, and HDAC8, which are most closely related to *Saccharomyces cerevisiae* transcription co-factor RPD3 and are involved in the regulation of transcription in the majority of vertebrate tissues. HDAC class II consists of HDAC4, HDAC5, HDAC6, HDAC7, HDAC9, and HDAC10 and is closely related to *Saccharomyces cerevisiae* histone deacetylase HDAC1. Members of HDAC class II are more tissue-restricted, compared to members of class I (de Ruijter et al. 2003). Sirtuins differ from HDACs class I and class II in catalysis of the reaction in which NAD^+ and an acetylated substrate are converted into a deacetylated product, nicotinamide, and O-acetyl ADP-ribose. This highly conserved mechanism is used in the regulation of chromatin organization, gene expression, cell cycle regulation, apoptosis and ageing (Grubisha et al. 2005). Members of all classes of HDACs were shown to participate in both targeted and non targeted genome-wide deacetylation of histones.

Several lines of evidence indicate that enzymes involved in histone acetylation and deacetylation (HATs and HDACs) participate in the establishment of cancer-specific transcription regulation. Chromosomal translocations and re-arrangements lead to the formation of genes coding for fusion proteins that interact with HATs and mistarget them to promoters of proliferative genes (Iyer et al., 2004). Nonfunctional HATs are created in Rubinstein-Taybi syndrome, which is linked to various malignances (Petrij et al., 1995; Eckner, 1996; McManus and Hendzel, 2001). Translocation 15/17 results in the fusion of the retinoic acid receptor alpha (*RARα*) gene with the promyelocytic leukaemia (*PML*) gene to form fusion proteins with PML, where RARα functions as a repressor (Lin et al., 2001). The acetylation status of chromatin can be increased by inhibition of HDACs by small molecules, such as trichostatin A (TSA), valproic acid, suberoylanilide hydroxamic acid (SAHA), and butyrate, which interfere with HDACs' enzymatic activity. Inhibition of histone deacetylases by HDAC inhibitors was shown to reverse several characteristics connected with the malignant phenotypes of cancers. TSA increases the radiosensitivity of glioblastoma cell lines (Kim et al., 2004). Inhibition of histone deacetylase activity by the HDAC inhibitor FK228 induces apoptosis and suppresses cell proliferation of human glioblastoma cells *in vitro* and *in vivo*. Sodium butyrate and TSA inhibit vascular endothelial growth factor (VEGF) secretion from human glioblastoma cells in cell cultures (Sawa et al., 2002, 2004). Another inhibitor of HDAC activity, 4-phenylbutyrate, modulates expression of glial fibrillary acidic protein and connexin 43, and enhances gap-junction communication in human glioblastoma cells (Asklund et al., 2004).

Searches in the ESTs have revealed an approximately 3-fold increase in incidence of most HDACs in brain tumours. HDAC3 has been found 3.1 times more often in brain tumours compared to non-tumorous brain tissue (de Ruijter et al., 2003). HDAC3 mediates the repressive function of unliganded thyroid hormone receptors (Ishizuka and Lazar, 2003) and can be bound to the thyroid hormone receptor in a ligand-independent manner, through the interaction with cyclin D1 (Lin et al., 2002). HDAC3 is also co-immunoprecipitated with HDAC4, 5, and 7 and forms a complex together with SMRT and NCoR (Fischle et al. 2001, 2002; Guenther et al. 2001).

In this work, we studied the expression of HDAC3 in glial tumours and benign glial tissues at the mRNA, protein and cell levels. We show that the expression of HDAC3 is elevated in glial tumours. High-grade gliomas (grade III and IV) also expressed more isoforms of HDAC3 compared to non-malignant tissues. While HDAC3 was found in normal glial cells and non-malignant gliosis exclusively as relatively weak and uniform nuclear/cytoplasmic staining, high-grade astrocytomas showed focally deregulated expression, consisting of strong cytoplasmic HDAC3 expression. Confocal microscopy showed co-localization of HDAC3 in nuclei visualized by DAPI in all examined tumours. Thus, elevated expression of HDAC3 may be indispensable for the growth of malignant human glial tumours.

Material and Methods

Biopsy samples

For this study, biopsy samples from 45 patients who had undergone therapeutic surgery for epileptic refractory lesions or brain tumours at the Department of Neurosurgery of the 1st Faculty of Medicine, Charles University and Central Military Hospital in Prague were used. This collection included 35 glial tumours, four non-malignant glioses removed for therapeutic purposes, one case of suspected glioma tissue (histologically classified as normal tissue but later a glioma was found in the vicinity of the previously removed tis-

sue), two meningeomas, two oligodendrogliomas and one lymphoma. Where possible, part of the material was frozen immediately after surgical removal and stored in liquid nitrogen. An informed consent for the use of the bioptic material was obtained from each patient prior to the study in accordance and with the approval of the Ethics Committee of the Central Military Hospital, Střešovice, Prague, and the Ethics Committee of the 1st Faculty of Medicine, Charles University and Faculty Hospital. Parallel formaldehyde-fixed paraffin-embedded (FFPE) biopsy material was processed for histopathologic examination and the diagnosis was established at the Department of Pathology, Central Military Hospital, Střešovice, Prague. Histopathologic diagnoses were established in accordance with WHO classification (Kleihues and Cavenee, 2000). All glial tumours included in this study are gliomas of astrocytic origin.

The frozen material was used to prepare frozen non-fixed sections in a Leica CM 1850 cryostat machine (Meyer Instruments, Houston, TX) and haematoxylin-eosin-stained sections, and for biochemical methods.

Extraction of nucleic acids and preparation of protein lysates

Sections of the frozen material were cut and collected in at least two pre-chilled eppendorf tubes (20 to 40 sections/tube). One tube was used for extraction of total RNA using RNA STAT 60 (Tel-Tex, Houston, TX) and the second tube was adjusted with 2x Laemmli buffer and a cocktail of protease inhibitors (Boehringer Mannheim, Mannheim, Germany) as recommended by the manufacturer. The quality of total RNA stained by ethidium bromide was controlled using agarose gel electrophoresis.

Reverse transcription

Five μg of total RNA were reverse transcribed with SuperScript II reverse transcriptase (Invitrogen, Carlsbad, CA) primed by random hexamers as recommended by the producer.

Amplification and characterization of HDAC3

Sequences of HDAC3 isoforms were retrieved from Genbank. Four transcripts were chosen from transcripts available in Genbank (April 10, 2006), three identical in CDS to isoforms originally reported by Yang et al. (1997) and an N-terminally deleted isoform. Sequences are represented by accession numbers:

1) AF039703.1 (CDS identical to U75697, originally denominated main isoform of HDAC3);
2) U75696.1 originally denominated HDAC3 isoform A (HDAC3A);
3) AF005482.1 originally denominated HDAC3 isoform C (HDAC3C);
4) AF130111.1 (a short isoform potentially coding for an N-terminally deleted protein) that we named isoform D (HDAC3D).

Since there are other nomenclatures of HDAC3 isoforms that recognize up to 13 transcripts (ACEview) and this study was not aimed at full characterization of expression of human HDAC3, we used the nomenclature of HDAC3 isoforms in keeping with the original description by Yang and coworkers (Yang et al., 1997) and added a new name for the N-terminally abrogated isoform as isoform HDAC3D. The primers for the amplification of specific regions of HDAC3 isoforms were (listed 5' –>3' as the sense and the antisense primers):

1) gttcatcttgtgtctccatcccga (HDAC3C sense)
2) catgtgccgcttccactccgagg (HDAC3, HDAC3A, HDAC3C sense)
3) ccaggatgccaatcacaatgtcgt (HDAC3, HDAC3A, HDAC3C antisense)
4) ttgctccttgcagagatgcgcct (HDAC3, HDAC3A, HDAC3C antisense)
5) gcattgacccatagcctggtcct (HDAC3 and HDAC3A sense)
6) gcctcagttacacatccaaactctaca (HDAC3C sense)
7) gaagtccactacctggttgataac (HDAC3, HDAC3A, HDAC3C, HDAC3D antisense)
8) aaactcgagccactcttaaatctccacatcg (HDAC3, HDAC3A, HDAC3C, HDAC3D antisense)

The primers for quantitative PCR were:

1) HDAC3 (all four isoforms): ccgaaatgttgcccgctgctg and aggtgcatggttcagcatctt
2) HDAC3+HDAC3A: acccatagcctggtcctgc and aggatgccaatcacaatg
3) HDAC3+HDAC3A+HDAC3C: gtgccgcttccactccga and aggatgccaatcacaatg
4) HDAC3D: ccgcctcagttacacatcca and tcatcaatgccatcccgc

Quantitative PCR was performed as described by Sun et al. (Sun et al., 2004) with modifications. Briefly, the amplicons for quantitative PCR of selected regions of HDAC isoforms were amplified using reverse transcription-PCR. The amplified fragments were eluted from agarose gels using electrophoresis and a semi-permeable membrane. The amount of DNA was determined spectrophotometrically. The purified DNA was used to determine the standard curves for each amplified region. Real-time PCR was preformed in PTC0200 DNA EngineR Thermal Cycler equipped with ALS0296 96+Well Sample Block and DyNAmoTM HS SYBRR Green qPCR Kit, which contains a hot start version of a modified Thermus brockians DNA polymerase to prevent extension of non-specifically bound primers during the reaction setup. The characterization of amplification included calculating the number of copies in samples using the computer program Opticon MonitorTM Version 3.0. Each sample was analysed at least two times. The number of copies was expressed in relation to the total RNA used for reverse transcription. The expression of glycerol-phosphate dehydrogenase,

β-tubulin and β-actin was determined in each sample with these primers:

1) GAPDH: ccgtctagaaaaacctgcc and gccaaattcgttgtcatacc
2) TUBB: atcagcaagatccgggaagag and ccgtgtctgacaccttgggt
3) ACTB: ccatcatgaagtgtgacgtgg and gtccgcctagaagcatttgcg

The primers were taken from RTPrimerDB Real Time PCR Primer and Probe Database (http:// medgen.ugent.be/rtprimerdb/index.php).

The amplified fragments were sequenced directly using an ABI Prism 3100 Avant (Applied Biosystems, Foster City, CA, USA) automated sequencer (kindly done by Ms. Helena Myšková in the sequencing facility of the Institute of Inherited Metabolic Disorders).

Western blot analysis

Western blots were performed using a standard protocol: samples were mixed with 2x Laemmli sample buffer (Laemmli, 1970) and 10x protease cocktail to reach 1x Laemmli sample buffer concentration and boiled for 7 min. Protein concentration was estimated using BCA Protein analysis kit (Pierce, Rockford, IL) as recommended. Thirty mg of protein were loaded for each sample, separated by electrophoresis and blotted onto a nitrocellulose membrane using a Mini Protean II apparatus (Bio-Rad, Hercules, CA). Remaining gels were stained by Coomassie blue. The membranes were then incubated in 1 % Tween 20 in phosphate-buffered saline pH 7.4 (T-PBS) containing 5 % (w/v) dried non-fat milk overnight at 4 ºC. The primary anti-HDAC3 antibody H3034 (Sigma, St. Louis, MO) was diluted 1 : 1000 in T-PBS containing 5 % (w/v) milk and the membranes were incubated for 1 h with this primary antibody at room temperature, washed six times in T-PBS for a total duration of 1 h and incubated with the goat anti-rabbit antibody labelled by horseradish peroxidase (Sigma) diluted 1 : 2000 in T-PBS for 1 h at room temperature and washed six times for a total of 1 h. After the wash in T-PBS, the secondary antibody was visualized using ECL-Plus chemiluminescent system (Amersham, Pharmacia, Uppsala, Sweden) or Supersignal purchased from Pierce.

Films were exposed from 10 s to 1 h and developed using an automated developer and analysed using NIH Image (Image J) program available on http://rsb.info.nih.gov/ij/.

Histological analysis

Standard FFPE tissue sections (7 μm) were dewaxed and hydrated according to the standard protocols.

U373 glioblastoma cells (a kind gift from prof. Alexi Šedo) were grown in DMEM containing 10 % FCS and gentamycin (100 μg/ml) in 5 % CO_2 humidified atmosphere. For histology, the cells were cultured in glass chambers as described (Mandys and Elleder, 1980) and fixed in 4 % paraformaldehyde for 5 min, cold acetone for 2 minutes, and stored dry.

Immunohistochemistry

The rabbit polyclonal anti-histone deacetylase 3 H3034 antibody (Sigma) used for detection of HDAC3 immunoreactive proteins was diluted 1 : 2000 in AntibodyDiluent (DAKO, Glostrup, Denmark). Secondary detection was performed using the horseradish peroxidase-labelled anti-rabbit IgG antibody, diluted 1 : 500, and visualized by the DAKO DAB system. Nuclei were stained by Weigert's haematoxylin.

Immunofluorescence

HDAC3 primary antibody was diluted 1 : 1000, secondary detection used the goat anti-rabbit IgG antibody labelled by Alexa Fluor 488 (Invitrogen-Molecular Probes, Carlsbad, CA) diluted 1 : 500 in TBS pH 7.6. For fluorescent detection, the nuclei were stained by DAPI (4'6-diamidino-2-phenylindole) diluted 1 : 1000 and added at the end of the procedure before mounting for 2 min. The staining protocol was the same for tissue sections and cultured cells.

Bright field, epifluorescence and laser scanning confocal microscopy

The slides were examined using an Olympus AX-70 microscope equipped with a DP-30 monochrome CCD camera and Analysis (Olympus, Tokyo, Japan) software for image acquisition. Complete available area of each sample was assessed. Three areas were selected for subjective evaluation of HDAC3 positivity. One area was selected for the highest staining pattern, one for the lowest staining pattern and one selected randomly. Each area was observed using a 40x objective, and all cells in the field scored for subjective positivity of HDAC3 staining in the bright field and epifluorescence illumination. Standard barrier filter sets were used for DAPI and Alexa Fluor 488 visualization. A Nikon Eclipse E400 microscope with a Cool Snap (RS Photometrics, Ontarion, NY) camera was also used for subjective evaluation of a complete set of samples by a second histologist.

A Nikon Eclipse TE2000-E microscope with C1*si* confocal head, Apo TIRF 60x (N.A. 1.49) objective and appropriate 450+/-15 and 515+/-15 band pass filter sets was used for confocal image acquisition. The image sampling density (*xyz*) was corrected to conform to the Nyquist criterion. The acquisition settings were kept constant for all image acquisitions except for a limited number of sections that had too weak or too intensive DAPI staining. The setting for HDAC3 recording was kept constant throughout the experiment. The overall evaluated volume from each sample was: four areas of 50 μm^2 (*xy*) were analysed in six consecutive 150 nm *z* steps with the maximum intensity plane in the middle. Sixteen cases that were available in paraffin-embedded sections and were also present in the collection exam-

ined biochemically were evaluated in three separate locations as complete *z* stacks consisting of 40 stacks averaged 10 times for both channels. The efficiency of used filter sets to prevent spectral cross-talk of DAPI and Alexa Fluor 488 was checked using the spectral mode and the linear unmixing algorithm of C1*si*.

Co-localization map construction

Co-localization maps using single pixel overlap coefficient values (in the range 0–1) (Manders et al., 1993) were calculated using Huygens Proffesional Software (SVI, Hilversum, The Netherlands) from representative maximum intensity *z* level *xy* sampled dual channel images. The overlap coefficient values were scaled with a lookup table (LUT) as demonstrated in Figs. 6 and 7. Prior to this analysis, non-specific background was subtracted from the DAPI channel of the images, and the images were again checked for potential spectral cross-talk. The background was also determined from the DAPI-stained sections that were processed without the primary antibody.

Results

I. Characterization of HDAC3 expression in non-malignant glial tissues and glial astrocytic tumours at the mRNA level

The *HDAC3* gene (NT_029289.10), which is localized on chromosome 5, spans 16770 bp and contains at least 15 exons. More than 380 partial sequences and 17 possible transcripts are deposited in public databases. There is evidence of existence of at least four types of HDAC3 transcripts that contain open reading frames (www.ncbi.nlm.nih.gov/sutilsevv.cgi?contig=NT029289.10&gene=HDAC3&lid=8841) (Fig. 1A). The HDAC3 isoforms deposited in databases can be represented by four sequences: the basic isoform, known as HDAC3 (Yang et al., 1997), which is represented in this work by AF039703.1 yielding a 1920 bp long open reading frame coding for a 428 amino acid protein with a calculated molecular weight of 48.8 kDa; HDAC3 isoform A (U75696.1) that has a 1941 bp long CDS, coding for a protein with 429 amino acids and a calculated molecular weight of 49.1 kDa; HDAC3 isoform C (AF005482.1) with 1981 bp long CDS, coding for a protein with 371 amino acids and a predicted molecular weight 42.3 kDa; and a short isoform lacking the N-terminal half of the CDS, represented by AF 130111.1. For the purpose of this study, we named the shortest isoform HDAC3 isoform D.

The coding region of isoform D starts in the 7th exon and uses the methionine that is present in all isoforms. The protein sequence derived from the open reading frame of isoform D is composed of 223 amino acids (calculated molecular weight 25.6 kDa) that form the C-terminal part of all remaining isoforms. Isoform D lacks the N-terminal sequence that was shown to be indispensable for histone-deacetylating function of HDACs (Zhang et al. 2005) (Fig. 1B).

We prepared a collection of four glial non-malignant tissues removed during therapeutic surgery, six low-grade gliomas and eleven high-grade gliomas (grades III and IV). Frozen sections were cut using a Leica Cryocut II apparatus and stored in eppendorf tubes. Total RNA was prepared and cDNA was made using Superscript II reverse transcriptase and random hexamers as primers.

Primers were designed to amplify HDAC3 and HDAC3A (from the start of a shared region to the stop codon), HDAC3C and HDAC3D. Similarly, primers for the amplification of the region common to all four isoforms were designed (Fig. 2A). Selected amplified sequences were characterized by direct sequencing and specificity of the amplification confirmed for all studied isoforms. Since the two longest isoforms are likely to be functionally similar if not identical, we searched for the expression of both HDAC3 and HDAC3A in all examined samples. PCR targeted to region B amplified the expected fragments from all examined samples and the specificity was confirmed by sequencing (Fig. 2).

Quantitative PCR directed at the region common to all four isoforms also amplified the expected fragments from all samples and the specificity of the amplification was confirmed by direct sequencing. For quantitative PCR, the standard curve for increasing number of copies per reaction was determined together with the assayed samples and the threshold set at the start of the efficient amplification. With the exception of one case that was histologically classified as grade II glioma, but was recurrent, all non-malignant glial tissues and grade II gliomas showed less than 10,000 copies per 150 ng of total RNA (Fig. 3A). Contrary to that, seven out of 11 gliomas of grade III and grade IV yielded more than 24,000 copies per 150 ng of total RNA (Fig. 3D). Interestingly, four of six examined gliomas of grade II had levels lower than those found in non-malignant tissue in 150 ng of total RNA.

Analysis of HDAC3 expression compared to the histological type of the examined tissues supported the elevated HDAC3 expression in high-grade gliomas (Fig. 3B). Expression of HDAC3 followed the expression of two housekeeping genes, glycerol 3-phosphate dehydrogenase, and β-actin, in keeping with the possibility that HDAC3 elevated expression is part of an overall disturbed expression profile in glial tumors. Normalization against β-tubulin alone followed the pattern of elevated HDAC3 expression in total RNA (Fig. 3C). The relative level of HDAC3 expression compared to β-tubulin also indicated elevated levels of HDAC3 in high-grade gliomas (Fig. 3D). A similar trend was observed for quantitative analysis of the expression of all three long isoforms or two longest isoforms (HDAC3 and HDAC3A), indicating expression of multiple isoforms of HDAC3 in high-grade gliomas.

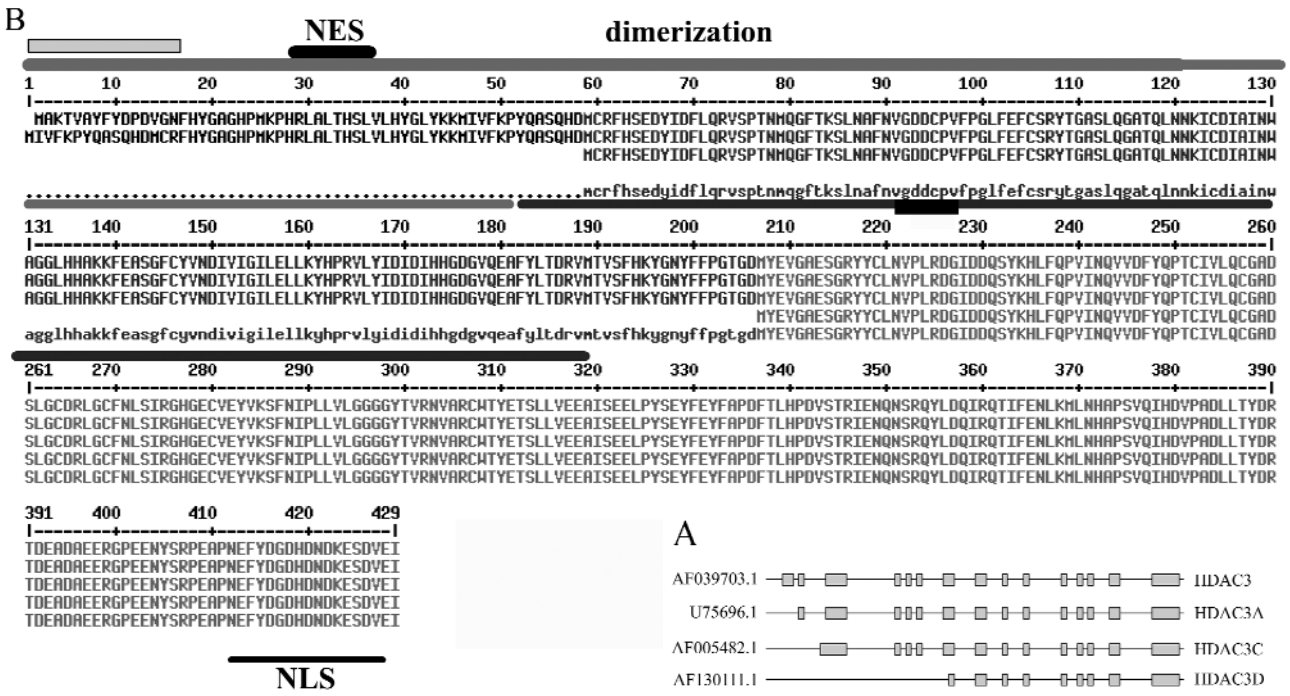

Fig. 1. A – Schematic representation of four isoforms of HDAC3 mRNA. Accession numbers and denomination used by Yang et al. (1997). B – Multiple alignments of proteins derived from mRNA shown in A. The sequences represent HDAC3, HDAC3A, HDAC3C and HDAC3D (from the top to the bottom). The bottom line shows the consensus calculated by the MultAline computer program. The sequence given in capital letters in the consensus line indicates the C-terminal part shared by all four isoforms. Note that HDAC3 and HDAC3A differ only in 15 or 16 N-terminal amino acids, respectively. HDAC3C starts at position 59 of HDAC3A and may differ in function since the N-terminal nuclear export sequence (NES) is missing in HDAC3C, but contains an additional nuclear export sequence (indicated by the dark bar in position 220–230) that is localized in the centre of the molecule. HDAC3, HDAC3A and HDAC3C may be expected to be functional deacetylases since both regions necessary for HDAC activity are present (Zhang et al., 2005; Zou et al., 2006). Contrary to that, HDAC3D lacks the N-terminal half of the molecule and is most likely a non-functional deacetylase. The C-terminus common to all four isoforms contains the nuclear localization signal (NLS).

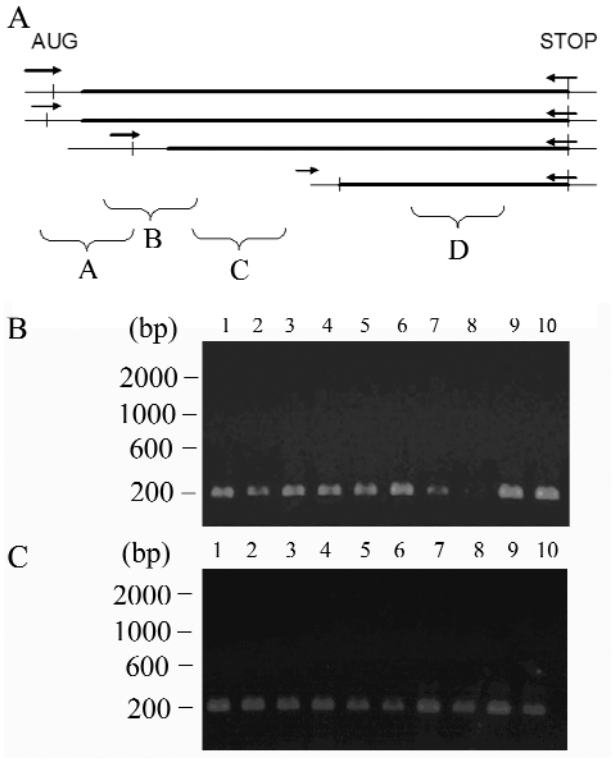

Fig. 2. A – Schematic representation of regions selected for quantitative PCR (regions A to D) and cloning of complete coding sequences of all four isoforms (arrows). B and C – Amplification of the region common to all three long isoforms (region C in panel A), showing the presence of these isoforms in all samples. Samples 1 to 10 correspond to cases coded as NCH 2, 3, 4, 5, 6, 7, 8, 9, 10, 11 (containing gliosis tissue – NCH3, as well as grade II – NCH 7, 8, 9 and grade IV gliomas – NCH 2, 4, 5, 10, 11) in panel B and NCH 17, 18, 19, 20, 21, 22, 24, 25, 26 and 27 (containing gliosis tissue – NCH 19, 20, 27, and low- – NCH 21, 22 – and high-grade gliomas – NCH 17, 18, 24, 25, 26) in panel C. The results indicate efficient amplification of region C indicated on panel A from all examined samples. The specificity of amplification was confirmed for selected cases by direct sequencing.

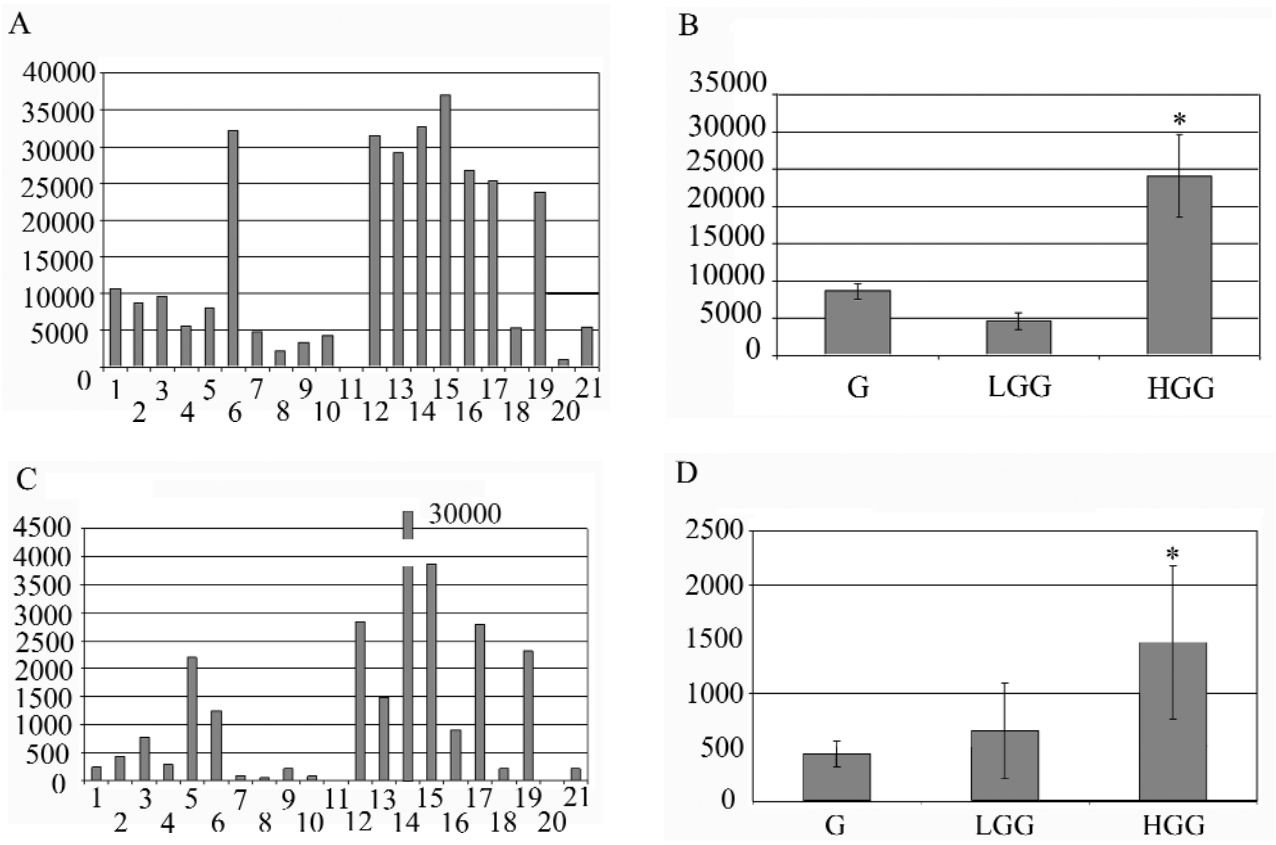

Fig. 3. Quantitative PCR for region D shown in panel Fig. 2A. Panels A and C show quantification of region D in cases numbered from 1 to 4 as follows: NCH 3, 19, 20, 27 (non-malignant gliosis), 5 to 10 low-grade gliomas NCH 6, 7, 8, 9, 21, 22, and 11 to 21 high-grade gliomas NCH 1, 2, 4, 5, 10, 11, 17, 18, 24, 25, 26. Bar 6 indicates a case with histological features of low-grade glioma, which was however recurrent. All values in this panel are expressed as calculated numbers of copies per 150 ng of total RNA. B – Quantification of HDAC3 mRNA expressed as average values in glioses (G), low-grade gliomas (LGG) and high-grade gliomas (HGG). Standard deviation is indicated. HGG show elevated values of HDAC3 mRNA compared to glioses and LGG at 95 % probability in Student's t-test. C – The same experiment as shown in panel A normalized for values found for β-tubulin mRNA. A similar trend as in readings normalized for total RNA is found. D – Average values and standard deviations calculated for the group of glioses, LGG and HGG from values normalized for β-tubulin (shown in C). Asterisk indicates values significantly different from values found in glioses and LGG at 95 % probability in the Student's t-test. The highest value obtained for case NCH 5 was not included in this calculation.

II. Detection of HDAC3 expression at the protein level by Western blot analysis

Western blot analysis with a rabbit polyclonal antibody revealed a faint band corresponding to a protein with an approximate size of 50 kDa in non-malignant glioses but prominent expression in tumour samples (Fig. 4A and B). Two non-malignant samples had a prominent band at 25 kDa (NCH19, 20) that presumably corresponds to a protein of N-terminally abrogated isoform D. On longer exposure films, a band with a size of approximately 58 kDa was also observed. Contrary to that, three out of five gliomas of grade II displayed 2-fold increased expression of the 50 kDa protein compared to the mean values seen in non-malignant samples (Fig. 5A) and two expressed a 25 kDa HDAC3 immunoreactive protein (Fig. 4A). All nine examined gliomas of grade III and IV expressed the 50 kDa HDAC3 and five of the nine gliomas had 2-fold the levels found in non-malignant tissue (Fig. 5A). Two samples contained a strongly expressed 48 kDa protein and a 42 kDa protein (Fig. 4B). Four out of nine cases had elevated levels of a 25 kDa protein. Densitometric analysis from two analyses prepared from the same material for each case revealed elevated expression of 38–50 kDa proteins (Fig. 5A) in high-grade tumours. Analysis of HDAC3/HDAC3A and HDAC3C expression related to the histological type of assayed tissue showed an increasing trend of HDAC3 expression in high-grade gliomas (Fig. 5B), indicating significantly elevated expression of the three longest isoforms in tumours and a trend for higher expression of HDAC3 in high-grade tumours. The result was significant in the Student's t-test with 95 % probability.

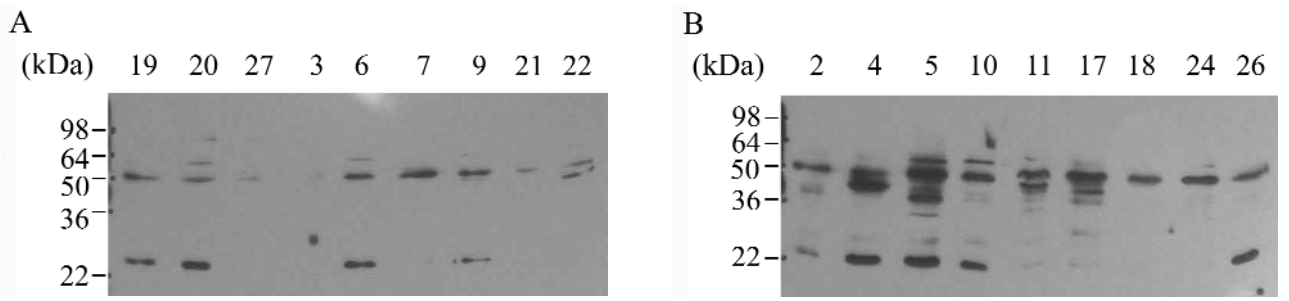

Fig. 4. Expression of HDAC3 detected by Western blot analysis. HDAC3 was detected by a rabbit polyclonal antibody specific for the C-terminus of the HDAC3 molecule. Panel A shows results obtained from non-malignant gliosis (cases NCH 19, 20, 27 and 3) and low-grade gliomas (cases 6, 7, 9, 21, 22) and panel B from high-grade gliomas (cases NCH 2, 4, 5 10, 11, 17, 18, 24 and 26). Tumours show higher expression of HDAC3 species in the range 48 to 54 kDa. HDAC3 expression is well visible in tumours and is strongly pronounced in the majority of high-grade gliomas.

In order to know whether HDAC3 is inherent to glial cells and not to other cell types that may contaminate the tumour samples, we studied HDAC3 expression in the cultured U373 human glioblastoma cell line. Quantitative PCR yielded values that corresponded to the highest values found in tumours. Similarly, HDAC3 at the protein level was found to be expressed in U373 cells as a prominent 50 kDa protein. Contrary to that, the 25 kDa protein was not observed in U373 cells despite the fact that the short isoform HDAC3D was amplified from U373 cells and confirmed by sequencing.

III. Analysis of HDAC3 expression at the cellular level

Thirty-five tumours were examined by histochemistry using the peroxidase method and by immunofluorescence. Immunohistochemistry detected HDAC3 weakly in the cytoplasm and nuclei in normal brain glial cells as well as in gliosis and low- and high-grade gliomas.

For an orientation analysis, all samples were evaluated as described in Methods. Cases where the observer classified 50 % of cells as cells containing cytoplasmic or nuclear staining that differed from control sections were classified as potentially HDAC3-positive. All evaluated tumours fulfilled this criterion.

For immunofluorescence, the samples were processed and evaluated as described in Methods. Non-malignant glial cells were weakly stained predominantly in the nuclei. Non-malignant gliosis showed stronger labelling for HDAC3 both in the nuclei and the cytoplasm. High-grade gliomas were strongly stained in the cytoplasm and had a pronounced focal character, containing areas with prominent cytoplasmic staining and areas with stronger nuclear HDAC3 localization. Although many fields examined were clearly characterized by observers as nuclear HDAC3 fluorescence,

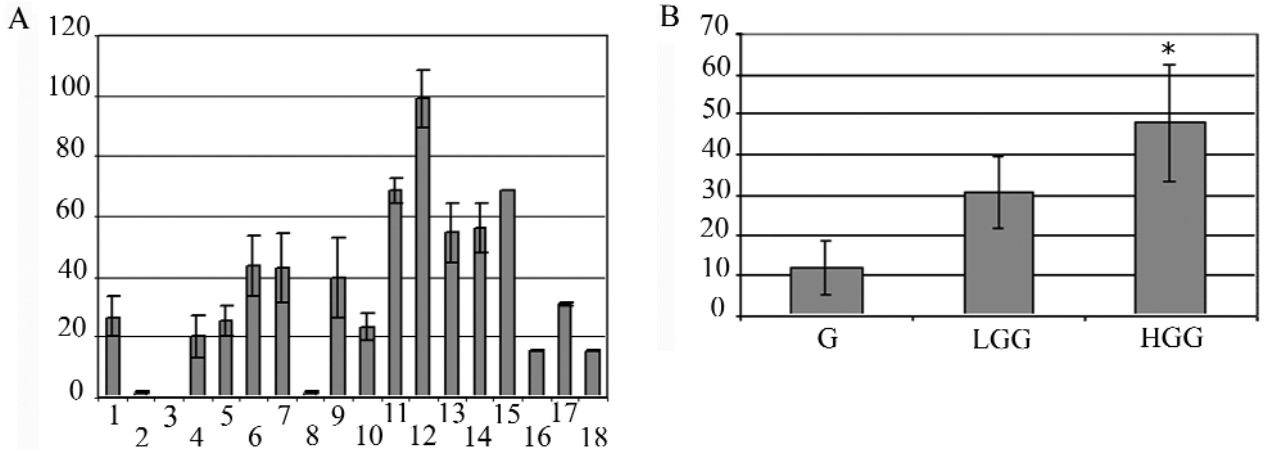

Fig. 5. A – Densitometric analysis of 48 to 54 kDa HDAC3 proteins in cases shown in Fig. 4. Values show mean and standard deviations of two independent Western blots. Bars numbered 1 to 18 correspond to cases NCH 19, 20, 27, 3 (G), 6, 7, 9 21, 22 (LGG), 2, 4, 5 10, 11, 17, 18, 24, and 26 (HGG) (as in Fig. 4).
B – Analysis of the average expression of HDAC3 in non-malignant gliosis (G), low-grade gliomas (LGG) and high-grade gliomas (HGG). The values found in high-grade gliomas are significant in the Student's t-test with 95 % probability.

a partial cross-talk from DAPI channel could not be excluded using the epifluorescence band pass filter sets. Analysis using the criterion of 50 % subjectively positive cells indicated that all cases of glial tumours were positive for HDAC3 staining.

Next, we analysed whether U373 cells showed staining for HDAC3 similar to the cells in the examined tumours. Epifluorescence detected HDAC3 in the cytoplasm of all cells. Nuclei were also stained but in some nuclear staining seemed to be compared to the cytoplasm (not shown).

Confocal microscopy

We employed confocal microscopy in order to evaluate the co-localization of HDAC3 staining with the nuclear compartment strongly labelled by DAPI. Analysis of U373 cells showed that HDAC3 staining was clearly detectable throughout the cytoplasm and was accumulated around the nucleus in many cells (Fig. 6A1 and B1). Nuclear staining was also clearly detectable (Fig. 6 A1 and B1). Co-localization maps (Fig. 6 A4 and B4) using single pixel overlap coefficient values were calculated as described in Material and Methods.

Co-localization maps revealed nuclear HDAC3 staining in all examined nuclei (Fig. 6A4).

Detection of HDAC3 expression in human glial tumors by confocal microscopy

A collection of samples that included all cases studied biochemically (except for three non-tumorous gliosis that were not available as paraffin-embedded material) was analysed as described in Methods. Analysis confirmed the HDAC3 expression pattern detected by immunohistochemistry and epifluorescence in the cytoplasm. A low and relatively uniform pattern was observed in normal glial tissue and in non-malignant gliosis, more intensive labelling in low-grade gliomas and strong focally accented labelling in high-grade gliomas. The nuclear labelling was also confirmed in all areas studied (Fig. 7 panels A1 to F1). Co-localization maps clearly showed nuclear localization of HDAC3 in all examined tumours (Fig. 7 panels A4 to F4).

Discussion

Our results show that HDAC3 is expressed at high levels in malignant human astrocytic glial tumours. HDAC3 was found to be expressed in multiple isoforms at both mRNA and protein levels. Four different transcripts are listed in the expert-curated NCBI database and more than 17 transcripts were found in more than 130 types of HDAC3 ESTs.

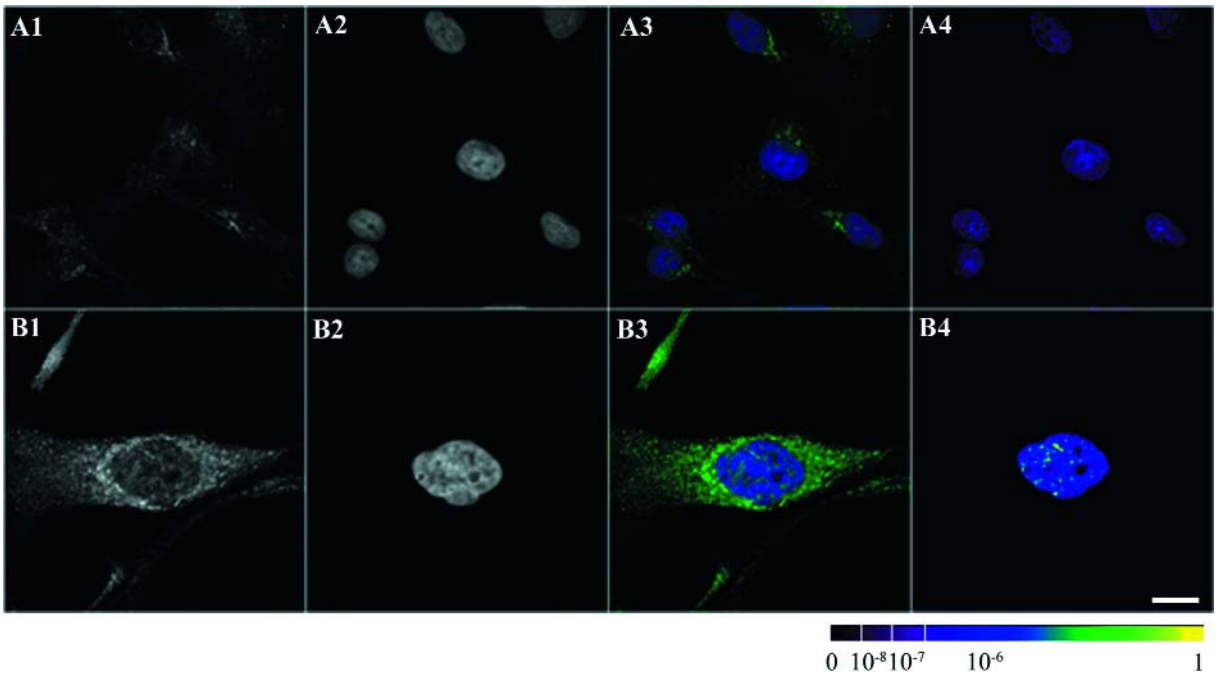

Fig. 6. Analysis of HDAC3 expression in U373 cells by immunofluorescence (confocal microscopy)
Panels A1 and B1 show representative planes of HDAC3 data acquisition as described in Methods, panels A2 and B2 show DAPI recordings, panels A3 and B3 show a simple merge view and panels A4 and B4 show the co-localization maps constructed as described in Methods. The lookup table (under the figure) represents values of a single pixel overlap coefficient, e.g. the contribution of each single pixel to the overall value of the overlap coefficient. Note that the overall image overlap coefficient value ranges from 0–1. The co-localization map shows every single pixel contribution to the overall overlap coefficient value scaled with an appropriate lookup table (refer to its scale beneath the Figure). This representation of the channel overlap is superior to the simple RGB merge for a number of reasons (e.g. single channel pixel intensity value inequity, etc.). Scale bar corresponds to 10 μm.

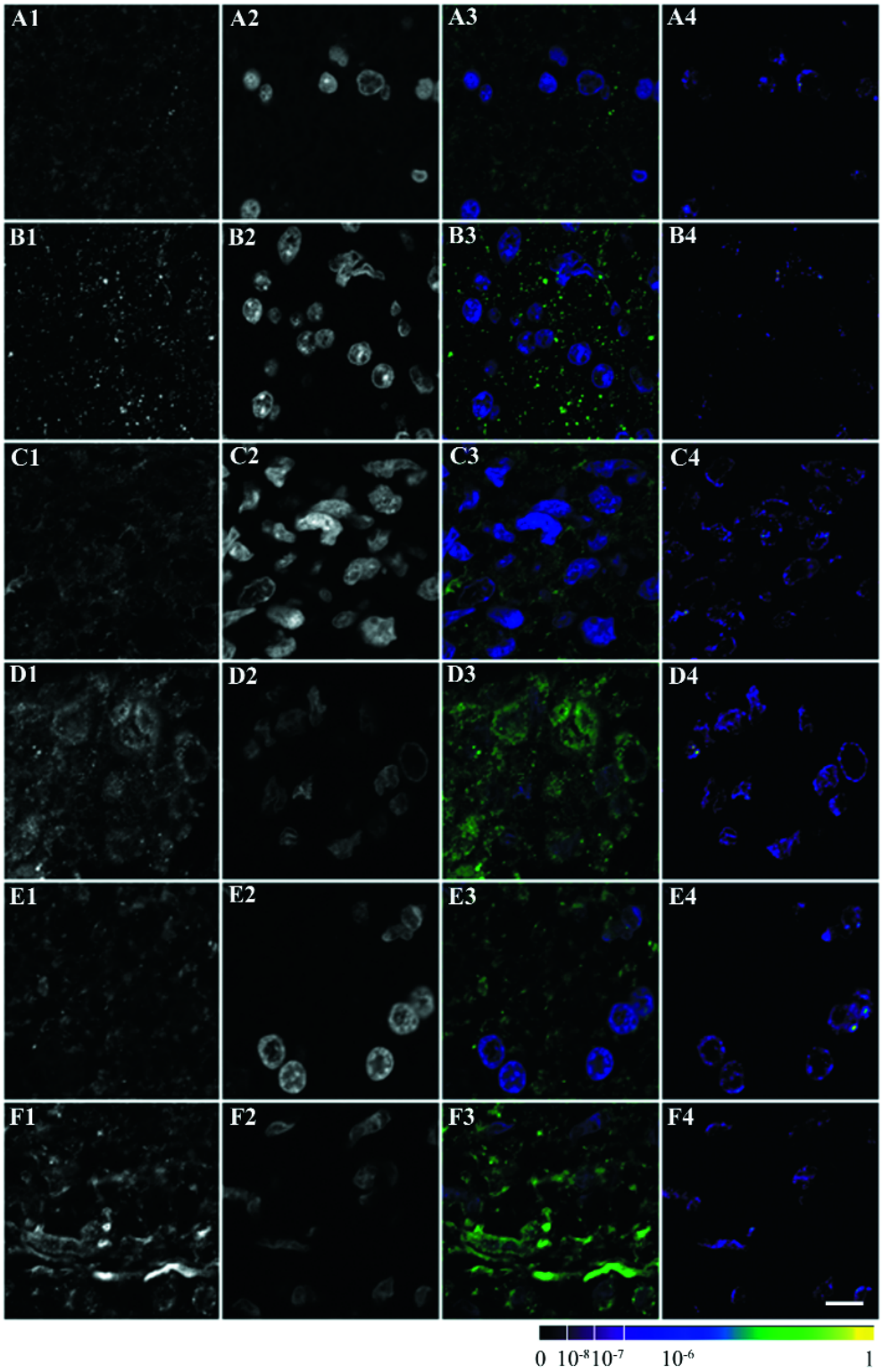

Fig. 7. Expression of HDAC3 in normal human glial tissue, non-tumorous gliosis and human glial tumours at the cellular level by confocal microscopy. Panels A1 to A4 show recordings from a standardized field in a sample from normal brain tissue, panels B1 to B4 show recordings from non-tumorous gliosis, panels C1 to C4 show recordings from low-grade glioma, panels D, E and F show recordings from three representative fields taken from the analysis of high-grade gliomas. Left panels (A1 to F1) show HDAC3 staining, panels A2 to F2 show DAPI detection and panels A3 to F3 show composite pictures. Panels A4 to F4 show co-localization maps calculated as described in Material and Methods and in legend to Fig. 6. While in normal glial tissue and gliosis the staining for HDAC3 is weak in intensity and uniform, the glioma shows strong cytoplasmic and nuclear staining, and the co-localization map clearly shows HDAC3 in the nucleus. Focal character of HDAC3 detection in high-grade gliomas is seen in panels D to F. Panels D1 to F1 show strong cytoplasmic detection of HDAC3. Co-localization maps show nuclear HDAC3 in all examined areas of high-grade gliomas (panels D4 to F4). Scale bar corresponds to 10 μm.

Originally reported HDAC3, HDAC3A and HDAC3C were amplified using specific primers and reverse transcription-PCR and their sequences confirmed by direct sequencing. Primers designed to amplify the N-terminally deleted HDAC3D mRNA led to the amplification of the expected fragment in one case but not in the remaining cases. HDAC3D was also found to be expressed in the U373 glioblastoma cell line at the mRNA level.

In keeping with the amplified cDNAs for the three long isoforms of HDAC3, Western blots detected proteins with sizes corresponding to the expected proteins derived from HDAC3, HDAC3A and HDAC3C. In some cases, a protein of approximately 25 kD was detected by HDAC3 C-terminus-specific antibody and can be expected to correspond to HDAC3D. In most cases that expressed this 25 kD protein, primers designed to amplify a 183 bp long fragment amplified longer fragments, ranging from 400 to 600 bp. Sequencing showed that at least in some cases, these fragments contained the coding sequence of HDAC3D.

Since HDAC3 and HDAC3A differ only in 15 or 16 amino acids, respectively, it is likely that their functions and cellular regulations are very similar if not identical. HDAC3C differs from the two longer isoforms by a deletion of 58 (57 compared to HDAC3A) N-terminal amino acids, but can be expected to be a functional HDAC based on a comparison with domains shown to be irreplaceable for the histone deacetylase function (Zhang et al., 2005; Zou et al., 2006). The shortest isoform, denominated HDAC3D, may correspond to the 25 kDa protein that is clearly recognized by Western blot in approximately one half of cases in this study. It is unlikely that HDAC3D is a functional histone deacetylase since it is missing domains necessary for histone deacetylase activity and can be expected to function as a negative regulator of some HDAC3 isoforms or even multiple histone deacetylases. Since our analyses failed to amplify the predicted cDNA of HDAC3D in several cases that expressed the 25 kDa protein recognized by HDAC3 antibody, its existence needs to be confirmed by direct proteomic methods.

The findings of this study indicate that the mRNA of HDAC3 is elevated in tissues of high-grade gliomas compared to non-malignant gliosis and low-grade gliomas. This was observed using quantitative PCR directed to amplify the region that is common to all four isoforms, three long isoforms and two longest isoforms from equal amounts of total RNA extracted from tissues. We interpret these findings as increased presence of HDAC3 in high-grade glioma tissues but not necessarily per cell or nucleus. The high expression of HDAC3 in malignant tumors was supported by the expression of HDAC3 at the protein level detected by Western blots.

Detection of HDAC3 by commercial antibodies and fluorescent microscopy (epifluorescence as well as confocal microscopy and co-localization analyses) show rather low nuclear expression of HDAC3 in histologically normal glial tissue. Contrary to that, gliomas, especially high-grade, showed strong cytoplasmic HDAC3 expression. Confocal microscopy and co-localization maps detected HDAC3 in the nuclei of an absolute majority of cells of glial tumours examined. Our data are in keeping with the possibility that HDAC3 may be indispensable for proliferation of glial cells and may play important roles in the malignant transformation of glial cells and growth of astrocytic tumours. This is supported by findings that inhibition of histone deacetylation by histone deacetylase inhibitor 4-phenylbutyrate exerts anti-proliferative and differentiation-inducing effects on a glioblastoma cell line that is connected with the induction of connexin 43 expression and inter-cellular communication via gap-junctions. Also, the non-phosporylated forms of connexin 43 and glial acidic fibrillary protein were induced by 4-phenylbutyrate (Asklund et al., 2004). HDAC3 is an effector in the transcription repression by thyroid receptors not occupied by a ligand (Ishizuka and Lazar, 2003). Cheng and coworkers (Lin et al., 2002) have shown that cyclin D1 can bring HDAC3 into the complex of thyroid receptors in a ligand-independent manner, thus overruling the transcription activation function of liganded thyroid receptors. Thus, the nuclear HDAC3 localization may be expected to have a potency to specifically inhibit a number of differentiation pathways.

An interesting feature observed in our experiments was the focal character of elevated cytoplasmic HDAC3 expression.

Histone deacetylases were shown to function not only in the nucleus, but also in the cytoplasm. HDAC inhibitors disrupt the complex between HDAC/protein phosphatase 1 (PP1) and in consequence dephosphorylation of Akt in U87MG glioblastoma and PC-3 prostate cancer cells. The HDAC inhibitors that were assayed differed in potency to activate the Akt dephosphorylation. TSA showed the highest effect compared to HDAC42 and SAHA (Chen et al., 2005). The proposed mechanism includes interaction of HDAC with PP1 in an active, phosphorylated form and excludes HDAC from interaction with other proteins, including Akt. Akt was shown to interact with HDAC1 and HDAC6 (Chen et al., 2005). HDAC3 activity, phosphorylation status and cellular localization were shown to depend on the interaction with PP4 (Gao et al., 2005). The activity is dependent not only on the phosporylation status, which may regulate the interaction of class II HDACs with 14-3-3 proteins (Grozinger and Schreiber, 2000; Bertos et al., 2001; Gagnon et al., 2003), but also on the activity of co-repressors of transcription factors (Guenther et al., 2001; Ishizuka and Lazar, 2003). It was shown recently that HDAC3 is also localized at the plasma membrane and may be phosphorylated by Src (Longworth and Laimins, 2006). HDAC3 expression, activity and cytoplasmic localiza-

tion is connected with tumour necrosis factor (TNF) signalling. HDAC3 inhibits the activation of MAPK11-mediated activating transcription factor-2 and expression of TNF (Mahlknecht et al., 2004). In the opposite way, regulation of nuclear translocation of HDAC3 by IκBα is required for the inhibition of PPARγ function by TNF (Gao et al., 2005).

In this study, we found HDAC3 in both nuclear and cytoplasmic localizations in all examined cases of high-grade gliomas. It can be speculated that the dual deregulated expression of HDAC3 may be important for biological properties of malignant gliomas.

Acknowledgement

Authors are grateful to M. Kolářová, F. Linx and L. Maršálková for technical assistance. We thank Prof. V. Beneš, and the staff of the Department of Neurosurgery, 1st Faculty of Medicine, Charles University and the Central Military Hospital, Prague, for the support throughout the course of this project.

References

Asklund, T., Appelskog, I. B., Ammerpohl, O., Ekstrom, T. J., Almqvist, P. M. (2004) Histone deacetylase inhibitor 4-phenylbutyrate modulates glial fibrillary acidic protein and connexin 43 expression, and enhances gap-junction communication, in human glioblastoma cells. *Eur. J. Cancer* **40**, 1073-1081.

Bertos, N. R., Wang, A. H., Yang, X. J. (2001) Class II histone deacetylases: structure, function, and regulation. *Biochem. Cell Biol*. **79**, 243-252.

Chen, C. S., Weng, S. C., Tseng, P. H., Lin, H. P. (2005) Histone acetylation-independent effect of histone deacetylase inhibitors on Akt through the reshuffling of protein phosphatase 1 complexes. *J. Biol. Chem.* **280**, 38879-38887.

de Ruijter, A. J., van Gennip, A. H., Caron, H. N., Kemp, S., van Kuilenburg, A. B. (2003) Histone deacetylases (HDACs): characterization of the classical HDAC family. *Biochem. J.* **370**, 737-749.

Eckner, R. (1996) p300 and CBP as transcriptional regulators and targets of oncogenic events. *Biol. Chem.* **377**, 685-688.

Fischle, W., Dequiedt, F., Fillion, M., Hendzel, M. J., Voelter, W., Verdin, E. (2001) Human HDAC7 histone deacetylase activity is associated with HDAC3 in vivo. *J. Biol. Chem.* **276**, 35826-35835.

Fischle, W., Dequiedt, F., Hendzel, M. J., Guenther, M. G., Lazar, M. A., Voelter, W., Verdin, E. (2002) Enzymatic activity associated with class II HDACs is dependent on a multiprotein complex containing HDAC3 and SMRT/N-CoR. *Mol. Cell* **9**, 45-57.

Fu, M., Wang, C., Zhang, X., Pestell, R. G. (2004) Acetylation of nuclear receptors in cellular growth and apoptosis. *Biochem. Pharmacol.* **68**, 1199-1208.

Gagnon, J., Shaker, S., Primeau, M., Hurtubise, A., Momparler, R. L.. (2003) Interaction of 5-aza-2'-deoxycytidine and depsipeptide on antineoplastic activity and activation of 14-3-3σ, E-cadherin and tissue inhibitor of metalloproteinase 3 expression in human breast carcinoma cells. *Anticancer Drugs* **14,** 193-202.

Gao, Z., He, Q., Peng, B., Chiao, P., Ye, J. (2005) Regulation of nuclear translocation of HDAC3 by IκBα is required for TNF-inhibition of PPARγ function. *J. Biol. Chem.* **281**, 4540-4547.

Grozinger, C. M., Schreiber, S. L. (2000) Regulation of histone deacetylase 4 and 5 and transcriptional activity by 14-3-3-dependent cellular localization. *Proc. Natl. Acad. Sci*. USA **97**, 7835-7840.

Grubisha, O., Smith, B. C., Denu, J. M. (2005) Small molecule regulation of Sir2 protein deacetylases. *FEBS J.* **272**, 4607-4616.

Guenther, M. G., Barak, O., Lazar, M. A. (2001) The SMRT and N-CoR corepressors are activating cofactors for histone deacetylase 3. *Mol. Cell Biol.* **21**, 6091-6101.

Heinzel, T., Lavinsky, R. M., Mullen, T. M., Soderstrom, M., Laherty, C. D., Torchia, J., Yang, W. M., Brard, G., Ngo, S. D., Davie, J. R., Seto, E., Eisenman, R. N., Rose, D. W., Glass, C. K., Rosenfeld, M. G. (1997) A complex containing N-CoR, mSin3 and histone deacetylase mediates transcriptional repression. *Nature* **387**, 43-48.

Higgs, D. R., Vernimmen, D., De Gobbi, M., Anguita, E., Hughes, J., Buckle, V., Iborra, F., Garrick, D., Wood, W. G. (2006) How transcriptional and epigenetic programmes are played out on an individual mammalian gene cluster during lineage commitment and differentiation. *Biochem. Soc. Symp.* 11-22.

Ishizuka, T., Lazar, M. A. (2003) The N-CoR/histone deacetylase 3 complex is required for repression by thyroid hormone receptor. *Mol. Cell Biol.* **23,** 5122-5131.

Iyer, N. G., Ozdag, H., Caldas, C. (2004) p300/CBP and cancer. *Oncogene* **23**, 4225-4231.

Jenuwein, T., Allis, C. D. (2001) Translating the histone code. *Science* **293**, 1074-1080.

Kim, J. H., Shin, J. H., Kim, I. H. (2004) Susceptibility and radiosensitization of human glioblastoma cells to trichostatin A, a histone deacetylase inhibitor. *Int. J. Radiat. Oncol. Biol. Phys.* **59**, 1174-1180.

Kioussis, D., Festenstein, R. (1997) Locus control regions: overcoming heterochromatin-induced gene inactivation in mammals. *Curr. Opin. Genet. Dev.* **7**, 614-619.

Kleihues, P., Cavenee, W. K. (2000). *World Health Orgnization Classification of Tumours of the Nervous System*. Lyon: WHO/IARC.

Laemmli, U. K. (1970) Cleavage of structural proteins during the assembly of the head of bacteriophage T4. *Nature* **227**, 680-685.

Lin, R. J., Sternsdorf, T., Tini, M., Evans, R. M. (2001) Transcriptional regulation in acute promyelocytic leukemia. *Oncogene* **20**, 7204-7215.

Lin, H. M., Zhao, L., Cheng, S. Y. (2002) Cyclin D1 is a ligand-independent Co-repressor for thyroid hormone receptors. *J. Biol. Chem.* **277**, 28733-28741.

Longworth, M. S., Laimins, L. A. (2006) Histone deacetylase 3 localizes to the plasma membrane and is a substrate of Src. *Oncogene*. Epub ahead of print.

Mahlknecht, U., Will, J., Varin, A., Hoelzer, D., Herbein, G. (2004) Histone deacetylase 3, a class I histone deacetylase, suppresses MAPK11-mediated activating transcription factor-2 activation and represses TNF gene expression. *J. Immunol.* 173, 3979-3990.

Manders, E. M. M., Verbeek, F. J., Aten, J. A. (1993) Measurement of co-localisation of objects in dual colour confocal images. *J. Microsc.* **169,** 375-382.

Mandys, V., Elleder, M. (1980) Demonstration of enzymes in cells cultured on semipermeable membrane in a double chamber. *Histochemistry* **65**, 325-327.

McManus, K. J., Hendzel, M. J. (2001) CBP, a transcriptional coactivator and acetyltransferase. *Biochem. Cell. Biol.* **79**, 253-266.

Nightingale, K. P., O'Neill, L. P., Turner, B. M. (2006) Histone modifications: signalling receptors and potential elements of a heritable epigenetic code. *Curr. Opin. Genet. Dev.* **16,** 125-136.

Petrij, F., Giles, R. H., Dauwerse, H. G., Saris, J. J., Hennekam, R. C., Masuno, M., Tommerup, N., van Ommen, G. J., Goodman, R. H., Peters, D. J., et al. (1995) Rubinstein-Taybi syndrome caused by mutations in the transcriptional co-activator CBP. *Nature* **376**, 348-351.

Sawa, H., Murakami, H., Ohshima, Y., Murakami, M., Yamazaki, I., Tamura Y., Mima, T., Satone, A., Ide, W., Hashimoto, I., Kamada, H. (2002) Histone deacetylase inhibitors such as sodium butyrate and trichostatin A inhibit vascular endothelial growth factor (VEGF) secretion from human glioblastoma cells. *Brain Tumor Pathol.* **19**, 77-81.

Sawa, H., Murakami, H., Kumagai, M., Nakasato, M., Yamauchi, S., Matsuyama, N., Tamura, Y., Satone, A., Ide, W., Hashimoto, I., Kamada, H. (2004) Histone deacetylase inhibitor, FK228, induces apoptosis and suppresses cell proliferation of human glioblastoma cells in vitro and in vivo. *Acta Neuropathol. (Berl)*. **107**, 523-531.

Sun, Y., Polishchuk, E. A., Radoja, U., Cullen, W. R. (2004) Identification and quantification of arsC genes in environmental samples by using real-time PCR. *J. Microbiol. Methods* **58**, 335-349.

Wolffe, A. P., Matzke, M. A. (1999) Epigenetics: regulation through repression. *Science* **286**, 481-486.

Yang, W. M., Yao, Y. L., Sun, J. M., Davie, J. R., Seto, E. (1997) Isolation and characterization of cDNAs corresponding to an additional member of the human histone deacetylase gene family. *J. Biol. Chem.* **272,** 28001-28007.

Zamir, I., Harding, H. P., Atkins, G. B., Horlein, A., Glass, C. K., Rosenfeld, M. G., Lazar, M. A. (1996) A nuclear hormone receptor corepressor mediates transcriptional silencing by receptors with distinct repression domains. *Mol. Cell. Biol.* **16**, 5458-5465.

Zhang, Y., Gilquin, B., Khochbin, S., Matthias, P. (2005) Two catalytic domains are required for protein deacetylation. *J. Biol. Chem.* **281,** 2401-2404.

Zou, H., Wu, Y., Navre, M., Sang, B. C.. (2006) Characterization of the two catalytic domains in histone deacetylase 6. *Biochem. Biophys. Res. Commun.* **341**, 45-50.